



## BEHAVIOUR OF CONCRETE - FILLED FRP CIRCULAR TUBES (CFFT)s SUBJECT TO COMBINED AXIAL COMPRESSION AND BENDING LOADS

Awad Mohamed El hashimy <sup>1</sup>, Magdy Mohammed Genedy <sup>1</sup>, Atef Elsayed Mohamed <sup>2</sup>,  
\*, Ahmed Mohamed Abou-Zied Tarkhan <sup>3</sup>

<sup>1</sup> Associative Professor of Properties and Strength of Materials, Department of Civil Engineering Faculty of Engineering - Mataria, Helwan University, Cairo, Egypt

<sup>2</sup> Ph.D. Candidate, Assistant Lecturer, Department of Civil Engineering Faculty of Engineering - Mataria, Helwan University, Cairo, Egypt

<sup>3</sup> Assistant Professor of RC. Structures, Department of civil Engineering Faculty of Engineering - Mataria, Helwan University, Cairo, Egypt

\*Corresponding author E-mail: Atefrehan41284@m-helwn.edu.eg

**Abstract.** This paper presents the results of an experimental study aimed at investigating the effect of important parameters on the behavior of circular concrete-filled fiber-reinforced polymer (FRP) tubes (CFFTs). The experimental program consisted of nine half-scale specimens that were constructed and tested to failure. The tested specimens were divided into two groups. The first group was composed of three plain concrete core tubes without outer confinement (PCTs) that were subjected to different levels of prestressing; there was also a control specimen. The second group consists of six CFFTs were confined with different FRP tube thicknesses and different levels of prestressing. All specimens had a circular cross section with a diameter of 200 mm and a total length of 2000 mm, which was tested in three-point bending over a simple supported span of 1800 mm. The studied parameters are the confinement effect of using FRP tubes, the FRP tube thickness and the effect of prestressing level. The test results showed that CFFTs can achieve substantially higher strength, serviceability, ductility, and energy absorption capacity than PCTs without FRP tubes. Furthermore, the significant effect of Prestressing is the activation of confinement mechanism of the concrete core restrained by the FRP tube.

**Keywords:** FRP, CFFTs, Concrete confinement and Prestressed concrete

## 1 Introduction

The construction field has shown significant need for innovative and long-lasting structural members. Fiber-reinforced-polymer (FRP) technologies provide a compelling option for confining concrete. Concrete-filled FRP tubes (CFFT) are a very effective kind of hybrid structural components used in sustainable building. The CFFT system combines the optimal qualities of FRP tube confinement, steel reinforcement, and concrete. CFFTs, often composed of glass or carbon FRP tubes, are filled with standard building materials like plain or reinforced concrete (RC) to create a hybrid composite high-performance structural system. This system is particularly well-suited for supporting heavy loads [1–4].

The FRP tube enhances the compressive load bearing capability and deformability of the concrete core by providing confinement. On the other hand, the concrete offers local stability to the thin-walled tube and thereby avoids early local buckling [5]. The FRP tube functions as both a permanent formwork for the concrete and a protective barrier against moisture and corrosive substances, so improving its durability [6]. Using FRP tubes instead of steel tubes has the benefit of precise control over the proportion of fibers in terms of thickness and the orientation of fibers in several directions. This allows for the efficient distribution of loads in both longitudinal and circular directions. The fibres in the circumferential direction are employed to provide confinement of the concrete, while the fibres in the longitudinal direction are utilized to offer the flexural strength and stiffness. Prestressed concrete is particularly beneficial to produce crack-free structural components and handle shrinkage and temperature effects. As a consequence, the ingress of damaging chemicals is pre-vented which aids in preventing reinforcement corrosion.

Cracking in concrete-filled tubes (CFT) may produce confinement deterioration, which leads in the lowering of strength, stiffness, and ductility in CFT beams. Therefore, adopting Prestress approach would completely activate the confinement mechanism and enhance the connection between the concrete and the FRP tube owing to compression stresses. Thus, increase the overall flexural performance of CFT beams. To the best knowledge of the authors', only two experimental studies have been re-ported in the literature to assess the effect of Prestress concrete-filled FRP circular tubes and rectangular steel tubes under pure bending [7,8].

Fam and Mandel [7] investigated five prestressed FRP CFFT circular beams under four-point bending. Test findings demonstrated that Prestress not only increases the strength and serviceability of the system but it also activates the confinement mechanism of the concrete core re- strained by the FRP tube. Flexural strengths and stiffnesses of pre- stressed FRP CFFTs may be enhanced by increasing tube thickness, choosing tubes with more longitudinal fibers, or increasing the number of strands.

Zhan et al. [8] examined the flexural performance of prestressed steel CFT rectangular beams. Eight prestressed CFST beams with a cross-section ( $300 \times 450$  mm) were tested. The effect of concrete strengths (50 and 60 MPa) and degree of Prestress (0.26 and 0.40) were examined. The test findings revealed that the prestressed strands delayed the fracture incidence and boosted the confinement effect of the core concrete, which, in turn, improved the composite action under bending. The cracking moment of prestressed steel CFT members was nearly 400% greater than that of non-prestressed steel CFT members. Based on these limited prior researches, adding Pre-stress for the CFFT may give many unique benefits, which would lead to great enhancement in strength, stiffness, deflections, and cracking control; and would make it a suitable alternative for high-performance structures. Despite its established benefits in terms of improving the structural behavior, there is currently a shortage of research investigations, for prestressed CFFT flexural components, especially with rectangular cross-sections. Moreover, there are essentially no code rules or guidance for the flexural design and serviceability of prestressed rectangular CFFT components. Therefore, the behavior of such members has yet to be established empirically and conceptually.

## 2 Experimental Program

### 2.1 Material Properties

**GFRP** tubes that were used in this study were locally fabricated at Delta Fiber Factory, 6 October Industrial Zone, Giza Province using the filament-winding manufacturing process as shown in **Fig. 1**, the tubes were made of E-glass woven roving and polyester resin with winding ply angle  $\pm 90^\circ$  respect to the longitudinal axis of tube. The glass fiber volume fraction was almost 51% laboratory determined. Tension standard tests were carried out according to standard test methods ASTM-638 [9] on nine identical samples to determine the tensile and mechanical properties in longitudinal (axial) and transverse (hoop) directions for the GFRP tubes, respectively. All GFRP coupons tested samples cross section were 40 mm x 2 mm and 300 mm length cut from the tubes. For all coupons samples, 50-mm end tabs were made of a mixture sand and iron filings to eliminate the effect of the tube's curvature and avoid sample slippage from testing machine grips. **Fig. 2** shows details of the test coupons. The mechanical properties of the GFRP tubes listed at **Table 1** and the axial stress-strain behavior obtained from coupon tests are shown in **Fig. 3**.



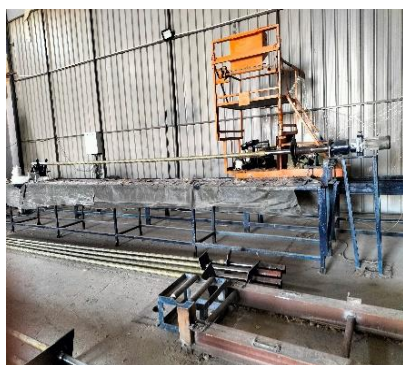
(a) E-glass fiber roving



(b) Fibers roving on creels



(c) Impregnation Fiber in



(d) Filament winding ma-

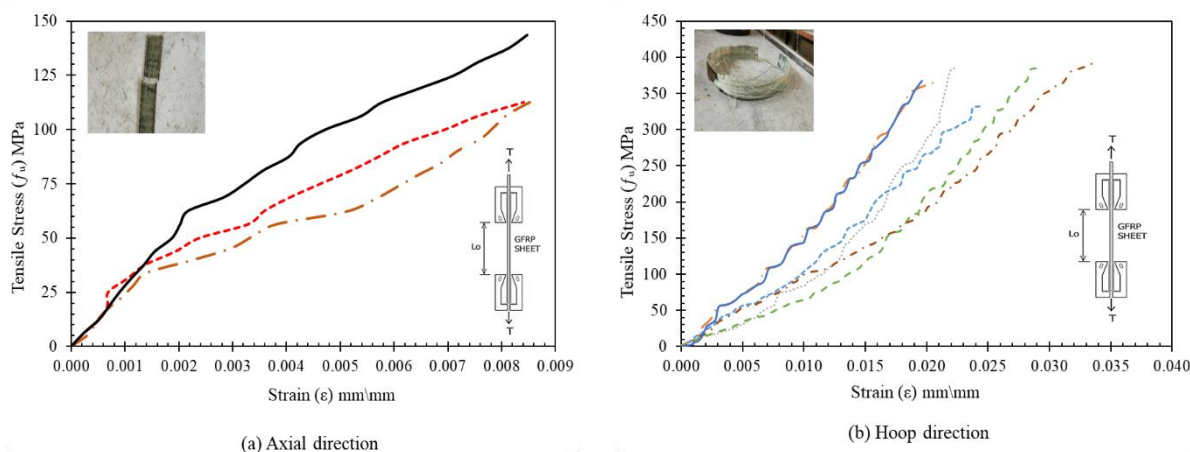


(e) GFRP tubes final product

**Fig. 1.** Manufacture GFRP tubes Filament winding process

**Table 1:** Mechanical properties of GFRP tubes

|  |         |
|--|---------|
| Inner tube diameter ( $D_{in}$ ) mm                  | 200     |
| Structure wall tubes thicknesses ( $t_f$ ) mm        | 2, 4, 6 |
| Axial tensile strength ( $f_{ta}$ ) MPa              | 119.7   |
| Elastic Modulus Axial ( $E_{fa}$ ) GPa               | 43.564  |
| Ultimate axial tensile strain ( $\epsilon_L$ ) mm/mm | 0.008   |
| Hoop tensile strength ( $f_{th}$ ) MPa               | 371.3   |
| Elastic Modulus Hoop ( $E_{fh}$ ) GPa                | 121.4   |
| Ultimate hoop tensile strain ( $\epsilon_L$ ) mm/mm  | 0.02    |

**Fig. 2.** Tensile test of GFRP coupon samples**Fig. 3.** Stress–strain behavior of GFRP tubes obtained from coupon tests

**Concrete** mix that was used for casting all specimens that are produced using a concrete mixer has a constant compressive strength. An average standard cube of 150 mm side length and equivalent standard cylinders of 150 mm  $\times$  300 mm were cast with tubes, cured in water, and tested after 28 days. The average characteristic cube and cylinder compressive strengths ( $f_{cu}$  and  $f'_c$ ) were 42.1 MPa and 32.1 MPa after 28 days, respectively. The concrete mix was produced from ordinary Portland cement, natural sand, crushed dolomite, with a maximum aggregate size of 10 mm. Superplasticizer of polycarboxylate-based high range water reducing admixture added to the mixture before casting the tubes to enhance the concrete workability.



## 2.2 Test matrix

A total of nine specimens half-scale-size circular tubes were casted and tested. Four specimens were created using GFRP tubes with the same structure wall thickness ( $t_f$ ) of 2 mm, while another two specimens were casted using GFRP tubes with differing structure wall thicknesses ( $t_f$ ) of 4 and 6 mm, respectively. The last remaining three control specimens were cast using PVC as a formwork and the tubes were removed before testing for comparison purposes. All tube specimens were 2000 mm long, with a circular cross-section and an inner diameter of 200 mm. The objectives of the study were to evaluate the effect of using GFRP tubes on the performance of axially pre-stressed CFFT beams and compare its behavior with its counterpart, plain concrete tubes, the GFRP tube thickness, and the axial pre-stressing percentage. **Table 2** provides a summary of all test specimens.


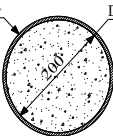
PVC pipes and GFRP tubes were used as formworks for the test specimens. For plain concrete specimens, PVC pipes of 200 mm inner diameter and 2000 mm height were cleaned and placed in a wooden frame likewise the GFRP tubes. The CFFT were casted handicraft from the top end in a vertical position to allow free consolidation of the concrete with minimal voids and internal vibration was also applied. **Fig. 4** shows mixing and casting the test specimens. After filling the tube, the top end was closed with flat plywood plate. The concrete-filled tubes were allowed to cure 20 days prior to testing.

The prestressing process of CFFT specimens as shown in **Fig. 5** was done with placing CFFTs between a set of two metal plates above and below the sample, and the sample was pressed from below using a hydraulic jack, allowing the lower plates to move with the hydraulic jack and securing the upper plates using a set of nuts. The sample was loaded with the required pressuring load for each sample as illustrated in **Table 2**. After reaching the required prestressing level, the set of nuts for the lower plates were tightened to ensure the pressure load effect continues during the sample testing under bending test.

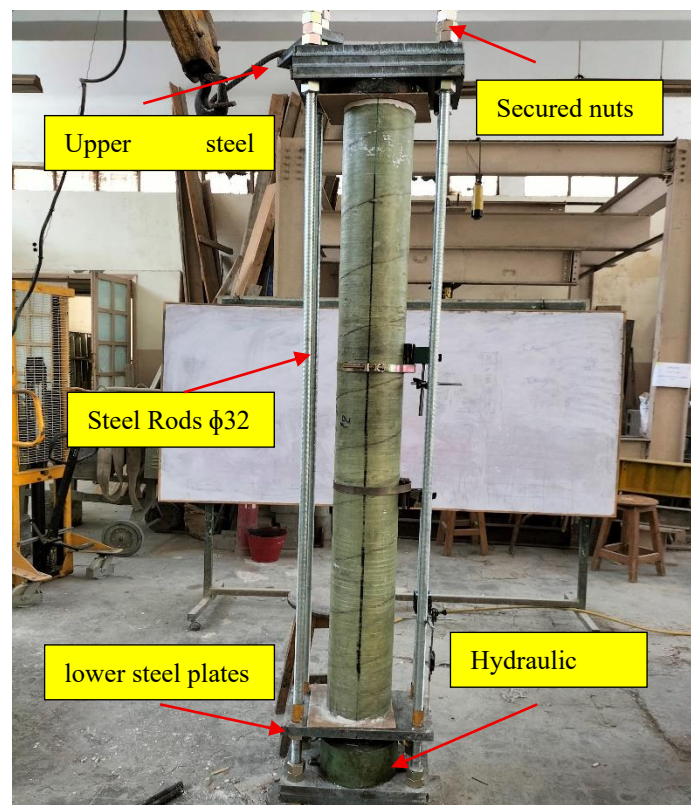


**Fig. 4.** Fabrication of test specimens

**Table 2:** Details of test specimens

| Group ID  | Test specimen | Cross section   | ( $t_f$ ) mm | Reinforcement ratio %<br>$\rho_f = (4t_f/D)$ | Pre-stressing ratio % (*) |
|---|---------------|---|--------------|--|---------------------------|
| <b>Group (1)</b><br><i>PCT-Control specimens</i>            | PCT-0%P       |  | ----         | ----   | ----                      |
|   | PCT1-25%P     |   |              |  | 25%                       |
|   | PCT2-50%P     |   |              |  | 50%                       |
| <b>Group (2)</b><br><i>Concrete-filled FRP tubes (CFFT)</i> | CFFT-0%P      |  | 2            | 4  | ----                      |
|   | CFFT1-25%P    |   |              |  | 25%                       |
|   | CFFT2-50%P    |   |              |  | 50%                       |
|   | CFFT3-75%P    |   | 4            | 8  | 75%                       |
|   | CFFT4-25%P-4  |   |              |  | 25%                       |
|   | CFFT5-25%P-6  |   |              |  | 25%                       |

\* Prestress ratio is referring to ultimate compressive strength of PCT specimen was tested under axial compression  
 $f_c$  (failure) = 29.92 Mpa

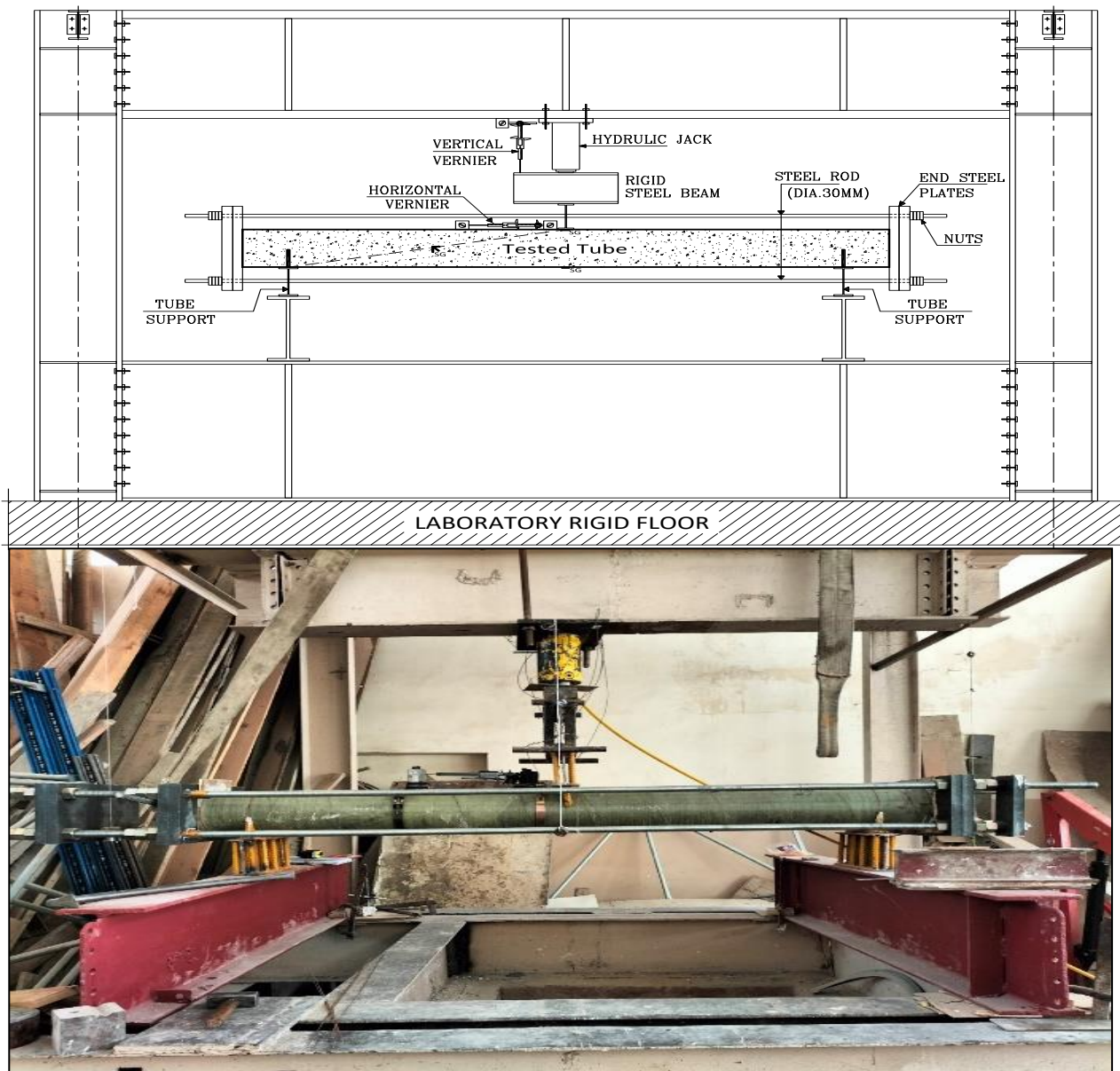


**Fig. 5.** Prestressing of CFFT of test specimens

### 2.3 Test setup and instrumentation

All specimens were tested through a rigid steel frame to determine the ultimate strength and deformation capacity. The specimens were tested using schematic three-point bending as simply supported members with a total length of 2000 mm and a clear span of 1800 mm. The static load was induced monotonically using a hydraulic jack and a load cell of 500 KN capacity, and the load was transferred to the loading point on the specimen through a rigid steel beam, as shown in **Fig. 6**.

A digital vernier caliper was used to monitor the mid span deflection and two another verniers were used for measuring strain at midspan were attached to the outer surface of the GFRP tubes for measure strain at hoop direction and axial direction.



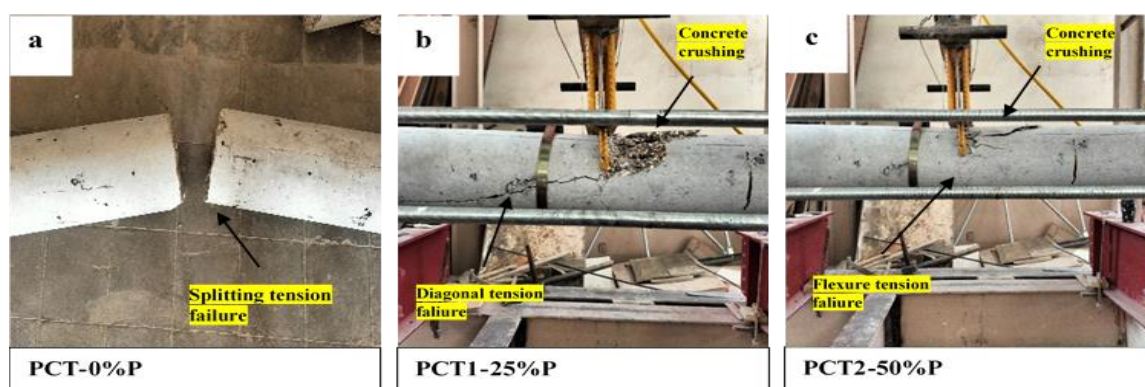
**Fig. 6.** Schematic for the setup used for testing the tubes



### 3 Test results and discussion

#### 3.1. Mode of failure

**Group 1**, concrete core tubes, the failure pattern of the tested tube PCT-0%P was a splitting tension-failure mode with tension crack fractures created at the soffit near the midspan under the point of application load as shown in **Fig. 7a**. The failure rapidly occurred as a result of the lack of tensile reinforcement and the pre-stressing load effect. The other specimens, PC1-25%P and PCT2-50%P, exhibit tension-compression failure as shown in **Fig. 7b and c**. At the early stage of loading, the tubes developed a flexure crack at the tension side of the tube at midspan. With higher loading levels, this crack gradually propagated till reaches almost the twice-third tube depth. Near the ultimate load, the tube compression flange had begun to be locally crushed at the top, reflecting the effect of tube axial pre-stressing. Furthermore, specimen PC1-25%P failure mode was accompanied by diagonal tension crack, during concrete compression flange crushing at top a diagonal tension crack at tube right side was propagated from the top of crushed concrete passing through the right support as shown in **Fig. 7b**.



**Fig. 7.** Group (1) Failure mode PC control specimens

**Group 2**, concrete- filled FRP tubes (CFFT), the failure pattern of tested tubes in this group also divided into two noticed failure modes, the first was a splitting tension failure mode that was indicated with rupture of the outer GFRP tube and a clear-cut fracture in the concrete core, this failure mode was noticed in specimen CFFT-0%P which was nearly a brittle failure almost also showed some ductility due to effect of concrete core confinement with GFRP tube, as well as the effect of the GFRP tube that act as longitudinal reinforcement but with low transverse stiffness as shown in as shown in **Fig 8a**. The second failure mode was flexure tension failure followed by crushing the concrete core and could be noticed for all CFFT prestressed specimens, the failure was started by cracking of concrete with reduction of specimen stiffness. As the load increases, the concrete is highly stressed in compression and tends to dilate excessively in the transverse direction as a result of GFRP tube confinement effect and pre-axial stress that acting on the specimen until the fibers rupture as shown in **Fig. 8b to 8f**. Insignificant micro surface cracks were formed in the GFRP wall tubes. However, the resulting cracks were very hard to be observed unless applying direct light on the tubes surface. Furthermore, flexure tension cracks formed on the GFRP tube shell during the loading of CFFT were accompanied by white patches that indicated flow of resin in the tube, leaving only white glass fibers to take the load as shown in **Fig 8f**. No slippage or relative movement was noticed between the tube and the concrete core at the end surfaces. This signified a complete interaction between them and their operation as one entity.



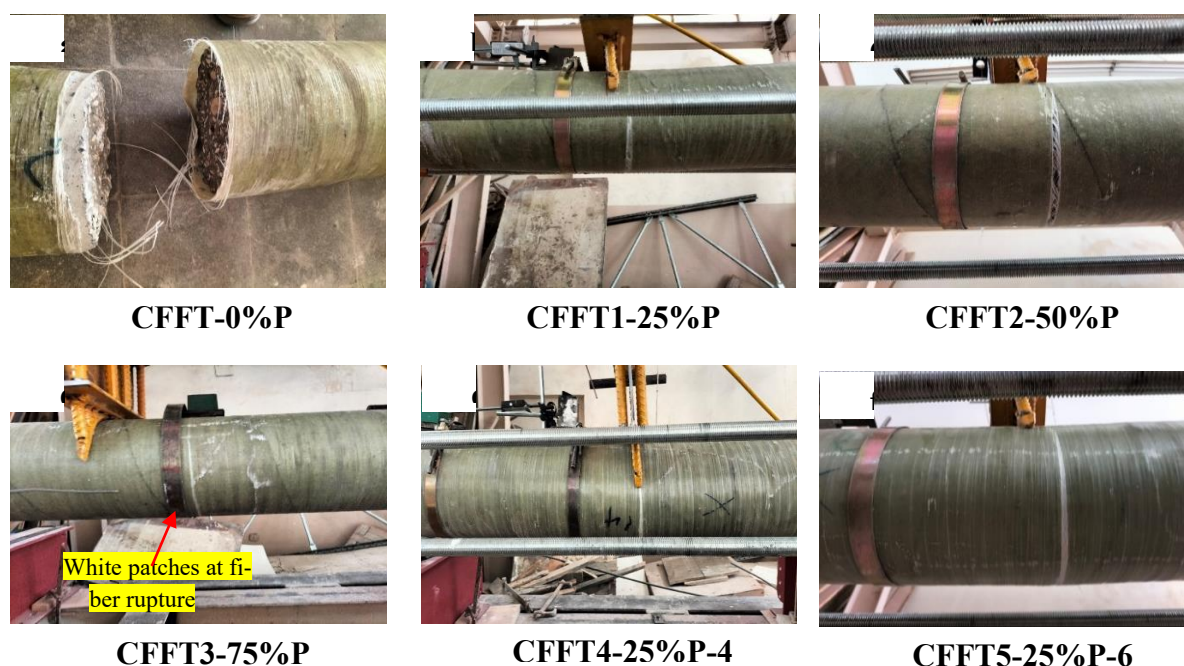


Fig. 8. Group (2) CFFT Failure modes

### 3.2. Load -deflection responses

During the initial loading stage in Group 1, specimens subjected to pre-axial compressive stress typically exhibit a bilinear load-deflection response until they reach the first crack load with minimal acquisition deflection. Subsequently, the load gradually increases with a noticeable increase in deflection, leading to a significantly non-linear behavior up to the failure load, as illustrated in **Fig. 9b and c**. The degree of non-linearity depends on the value of axial precompression stress that affects the tubes, and evidently, the tube specimen PCT2-50% is more likely to exhibit non-linear behavior than the tube PCT1-1P-25% since it was prestressed axially with 15.10 MPa. Whereas PCT1-25% is affected by 7.55 MPa, as shown in **Fig. 9d**.

The failure load for PCT1-25%P was 63.5 KN, while for PCT2-50%P, it was 85.7 KN, an increase of about 35%. The specimen PCT-0%P load-deflection curve was exhibiting almost bilinear behavior as a characteristic of the plain concrete core, as shown in **Fig. 9a**. The failure load was 6.3 KN is relatively low compared with earlier samples as shown in **Fig. 9d**. That's because there is no longitudinal reinforcement or axial precompression stress.

Table 3: Summary of test results

| Group ID  | Test specimen       | Failure load $P_f$ (KN) | Ultimate deflection $\Delta_u$ (mm) | Total energy absorbed $E_{TOT}$ (KN.mm) |
|---|---------------------|-------------------------|-------------------------------------|---|
| <b>Group (1)</b><br>PCT- Control specimens            | <i>PCT-0%P</i>      | 6.3                     | 1.5                                 | 5.95                                    |
|   | <i>PCT1-25%P</i>    | 63.5                    | 17.33                               | 637                                     |
|   | <i>PCT2-50%P</i>    | 85.7                    | 18.07                               | 902                                     |
| <b>Group (2)</b><br>Concrete- filled FRP tubes (CFFT) | <i>CFFT-0%P</i>     | 9.6                     | 2.22                                | 13.8                                    |
|   | <i>CFFT1-25%P</i>   | 84.3                    | 26.51                               | 1506                                    |
|   | <i>CFFT2-50%P</i>   | 111                     | 28.95                               | 2093                                    |
|   | <i>CFFT3-75%P</i>   | 165.5                   | 31.5                                | 3313                                    |
|   | <i>CFFT6-25%P-4</i> | 102                     | 34                                  | 2318                                    |
|   | <i>CFFT7-25%P-6</i> | 122.5                   | 35.15                               | 2732                                    |

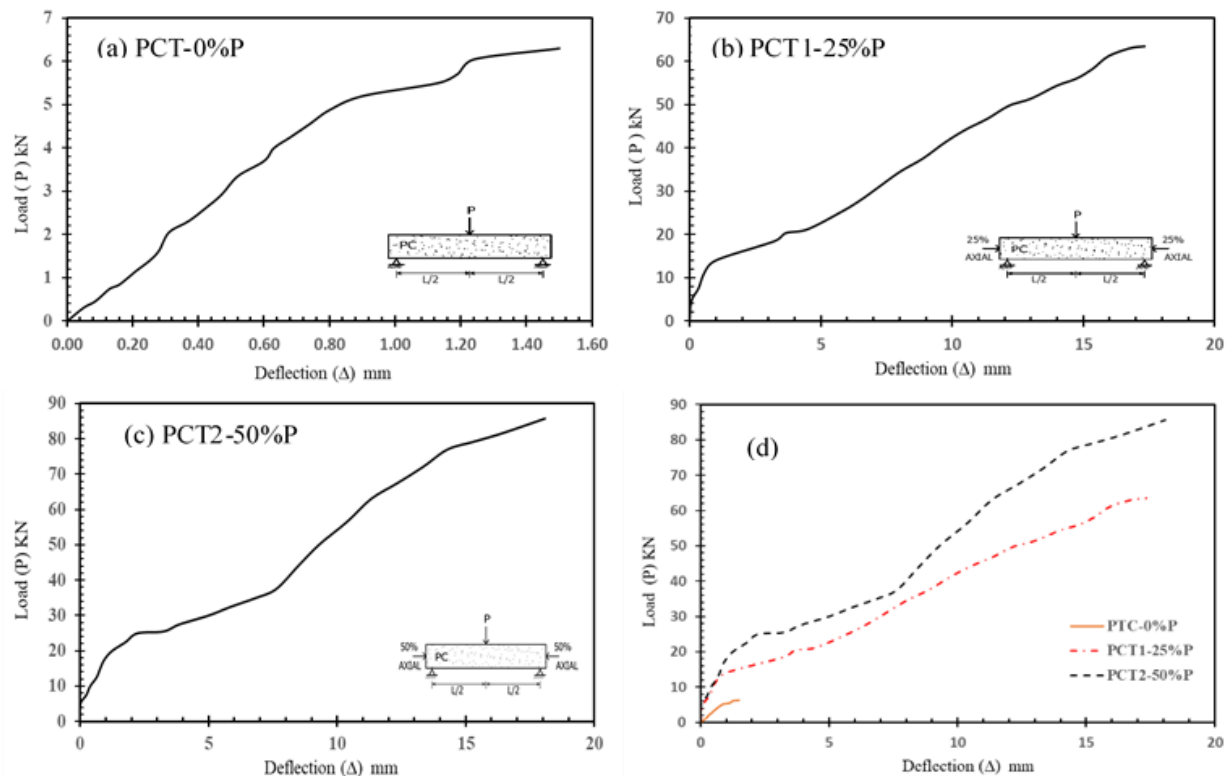


Fig. 9. Load-deflection curve of Group (1) PC control specimens

In general, all Group 2 CFFT specimens exhibited bilinear behavior at the early stage of loading until cracking the concrete core, reflecting the influence of axial Prestressing load on the specimens. Following a reduction in tube stiffness as shown in *Fig. 10g*. Increasing the load in the presence of confinement induced by the GFRP tube, the tested samples behaved in a bilinear manner until the failure load, as shown in *Fig. 10b, c, d and f*, except for CFFT-0%P, which exhibits non-linear behavior until failure as shown in *Fig. 10a*.

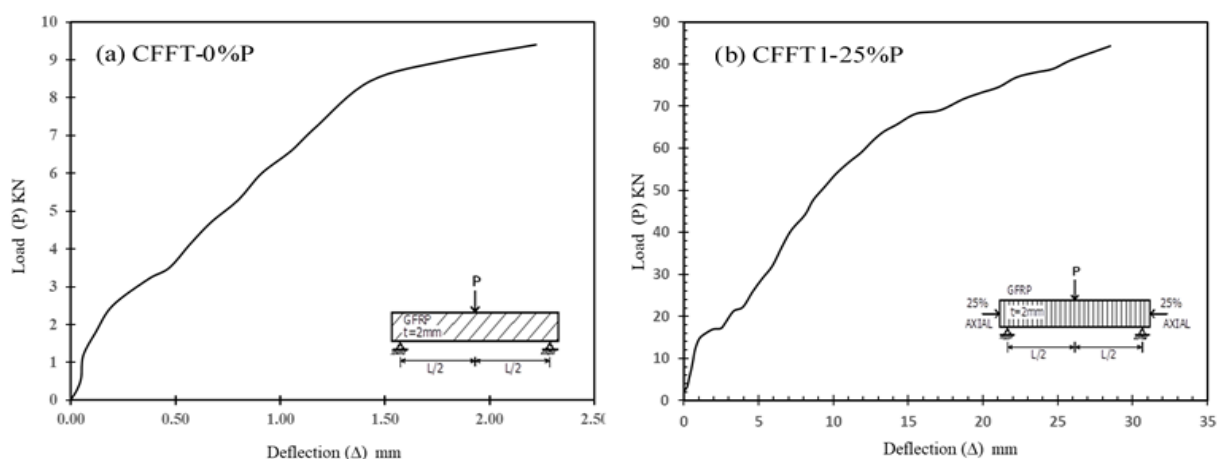


Fig. 10. Load-deflection curve of Group (2) CFFT specimens

CFFT1-25%P CFFT2-50%P and CFFT3-75%P which have the same tube thickness, had failure loads of 84.3 KN, 111 KN and 165.6 KN, respectively. Furthermore, the failure loads of CFFT4-25%P-4 and CFFT5-25%P-6 were 102 KN and 120.6 KN, respectively, as a result of tube thicknesses differences. The failure load of CFFT-0%P was slightly higher than that of the specimen PCT-0%P (9.60 KN) as a result of the GFRP tube that provides concrete confinement and reinforcement to the concrete core.

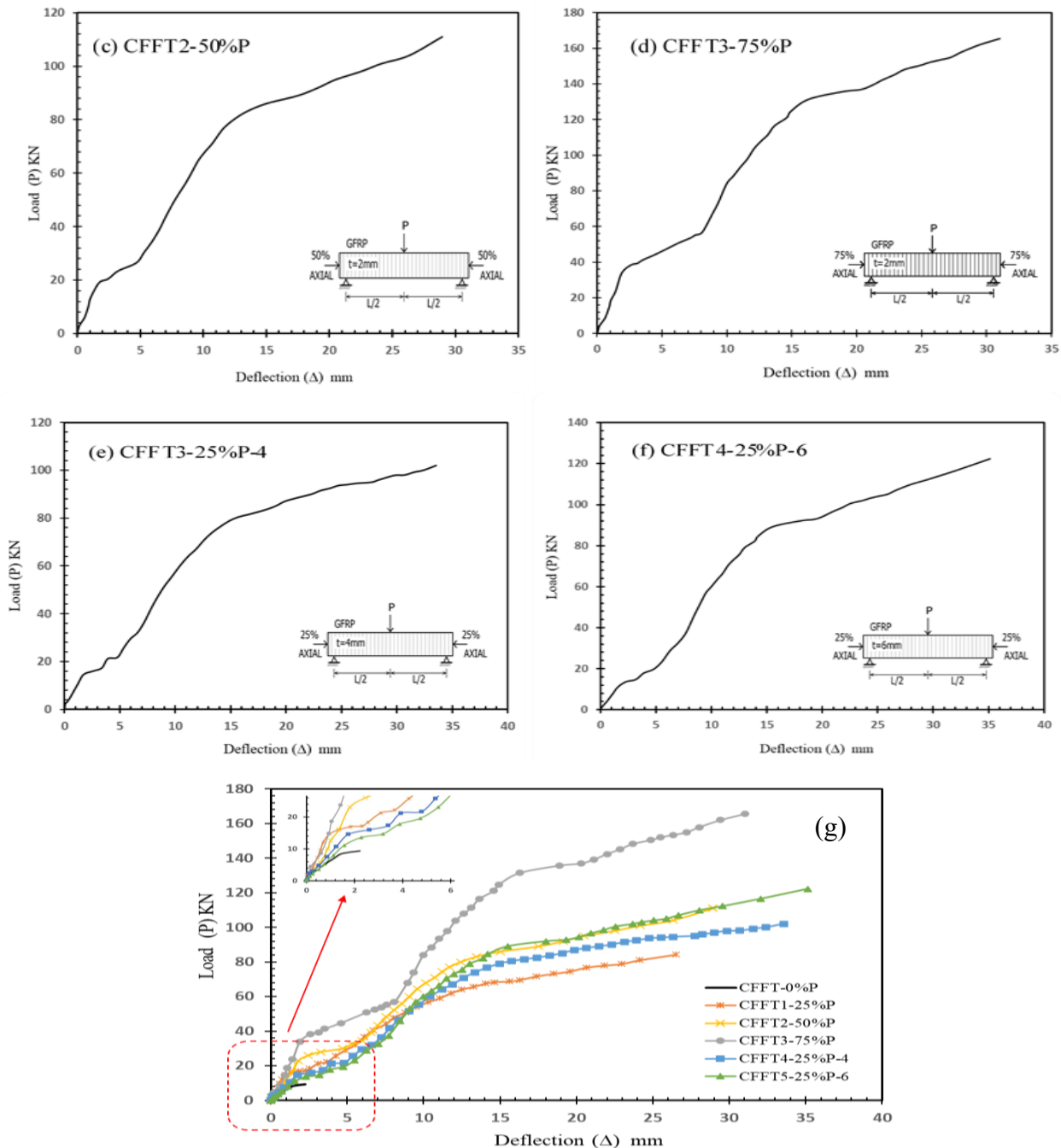
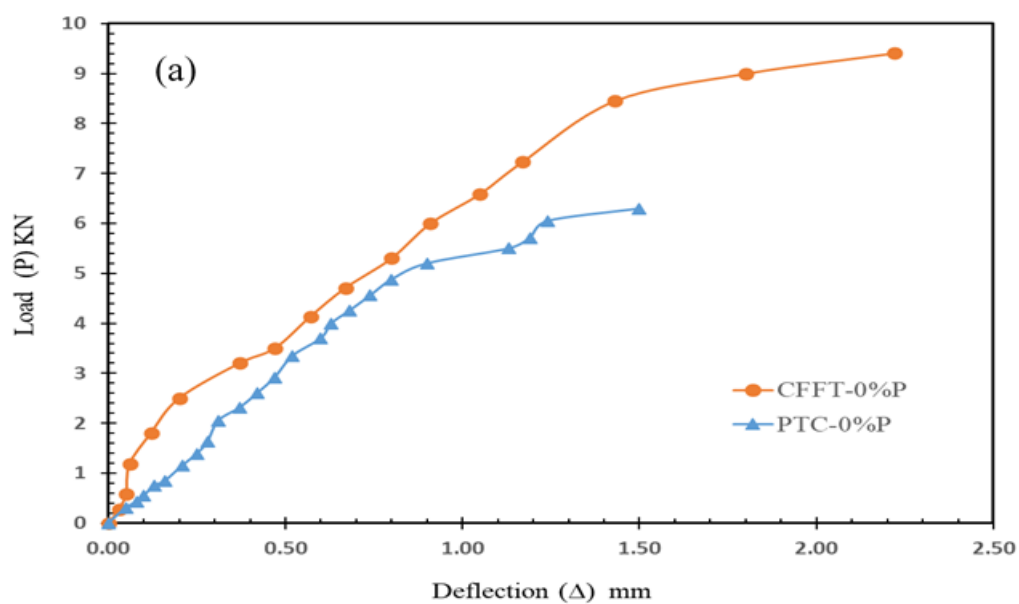


Fig. 10. (cont.) Load-deflection curve of Group (2) CFFT specimens

### 3.3. Effect of GFRP tube

Comparing the behavior of the PCT specimens in group (1) with the counterpart CFFTs in group (2), we could clearly see the effect of the GFRP tube. GFRP tube that was installed in specimen CFFT-0%P increased the ultimate load by 52.4% compared to that of PCT-0%P. Furthermore, increasing its stiffness, as shown in *Fig. 11a*, the same occurred in CFFTs that were subjected to axial pre-compressive stress; the ultimate load of CFFT1-25%P and CFFT2-50%P increased by 32.8% and 29.5% compared to that of PCT1-25%P and PCT2-50%P, respectively, as shown in *Fig. 11b*. We can say that confining the concrete with FRP tubes can provide more strength and ductility, not only that it



inhibits concrete core instability from local buckling and deterioration and compression failure.

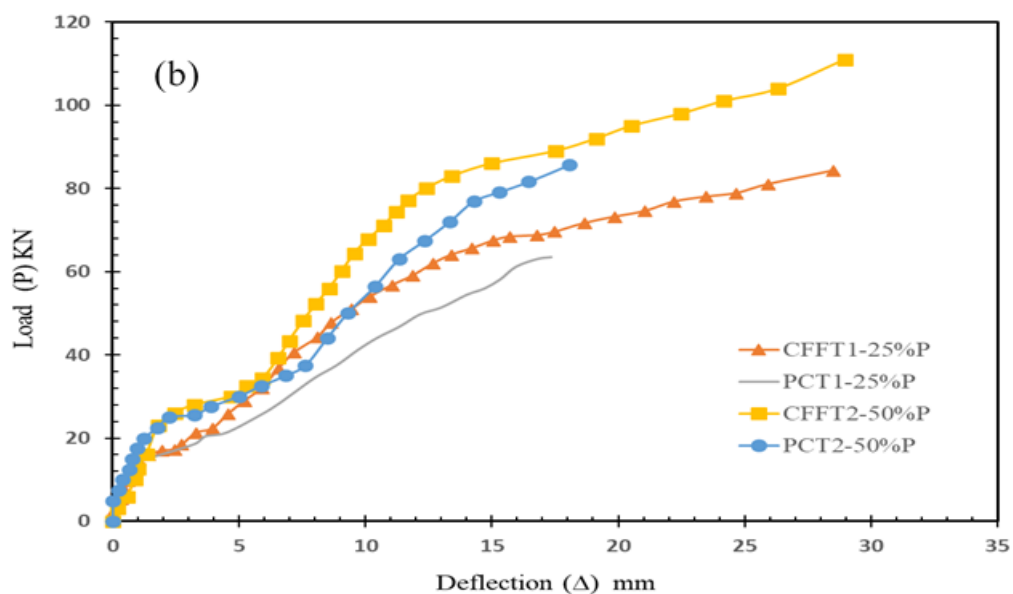


Fig. 11. Effect of GFRP tube

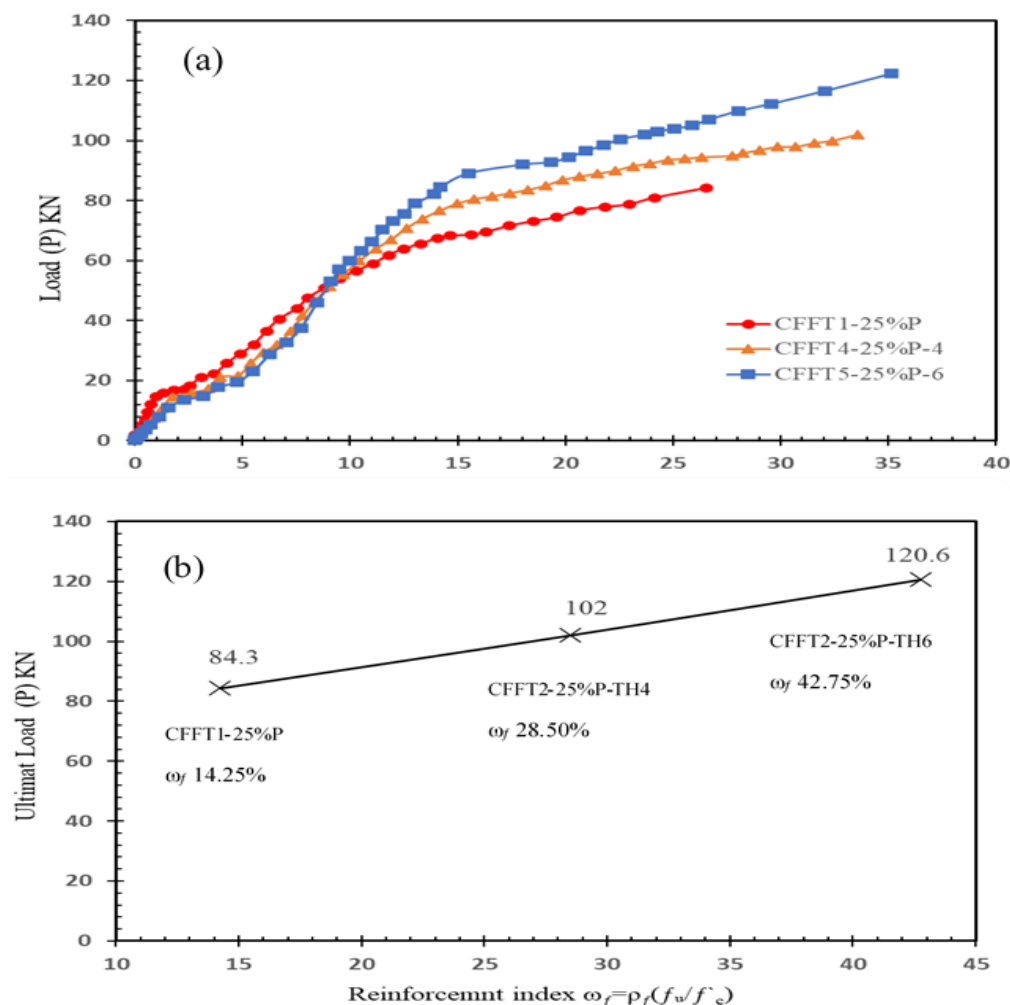


### 3.4. Effect of GFRP tube thickness ( $t_f$ )

The thickness of the FRP tube structure wall ( $t_f$ ) has a significant impact on the CFFT strength. It can be noticed in the tested specimens in our study, that by increasing the fiber tube thickness in CFFT1-25%P from 2mm to 4mm and 6mm in CFFT4-25%P-4 and CFFT5-25%P-6, respectively, the ultimate load increased by 21% and 45.3% as shown in **Fig. 12a**. The effect of FRP tube thickness not only affects the ultimate strength of CFFT from the point of view of the confining concrete core but also its contribution as a type of reinforcement in the hoop and longitudinal directions of the tubes. The reinforcement index ( $\omega_f$ ) had been expressed to explain this effect Eq (1), as shown in **Fig.12b**. The CFFTs ultimate load increased sequentially as reinforcement index ( $\omega_f$ ) increased.

$$\omega_f = \rho_f (f_u / f'_c) \quad (1)$$

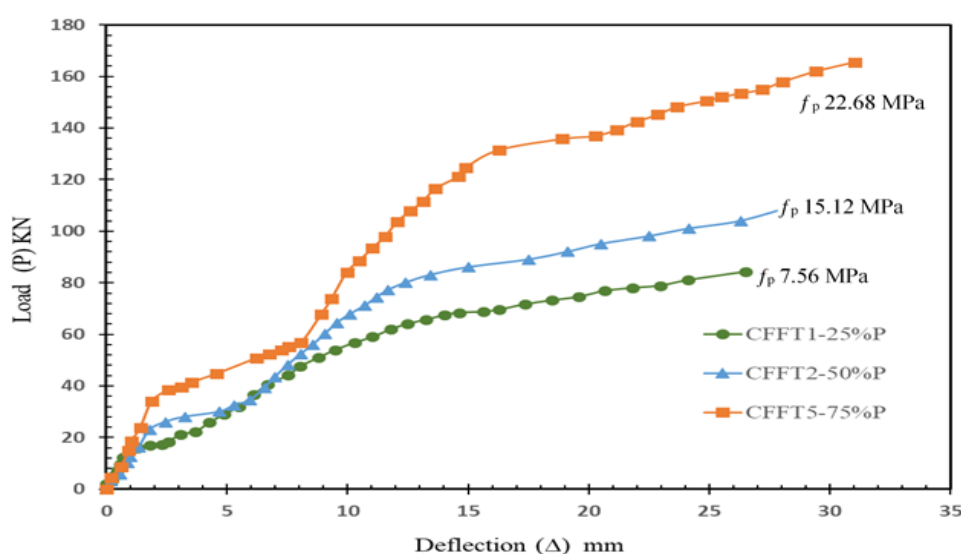
( $\rho_f$ ) is the FRP ratio equal ( $4t_f/D$ ), ( $f_u$ ) tensile strength of GFRP and ( $f'_c$ ) concrete compressive strength.



**Fig. 12.** Effect of GFRP tube thickness ( $t_f$ )

### 3.5. Effect of prestress level on flexure response and confinement

The load deflection responses of specimens CFFT1, CFFT2, and CFFT3 are compared to observe the impact of prestressing on their behavior as shown in **Fig. 13a**, the prestress levels in the concrete of the mentioned specimens were 7.56 MPa, 15.12 MPa, and 22.68 MPa, respectively. The curves indicate that the difference in prestressing level has a moderate effect on initial stiffness before cracking but has a significant effect on the ultimate loads and deflections, specially at high level of prestressing, it can be noticed from the ultimate failure load of specimens CFFT1-25%, CFFT2-50% and CFFT3-75% that increased by 878%, 1156% and 1724% respectively, by increasing prestress levels. The values of deflection also got better and decreased at high prestressing levels, the ultimate beam deflections of CFFT1, CFFT2 and CFFT3 were 26.51mm, 28.95 mm and 31.5 mm, respectively.



**Fig. 13a.** Effect of prestress level on flexure response of CFFTs

To examine the effect of prestress level on concrete confinement, the hoop-axial strain response of tested CFFTs should be compared, as shown in **Fig. 13b**. As the axial strain increases, the hoop strain increases at a higher rate of prestressing level. The CFFT5 hoop strain at failure was 0.005, which is higher than measured at specimens CFFT1 and CFFT2, which were 0.002 and 0.0036, respectively, which indicate high effective concrete confinement. An expression of confinement index ( $\theta_f/\theta_i$ ) had been derived to assess the confinement level as affected by prestressing level ( $f_p$ ), **Fig. 13c** show the variation of confinement index with ( $f_p$ ) the increase in confinement index reflects an increase in concrete compressive strength as the prestress level increase.

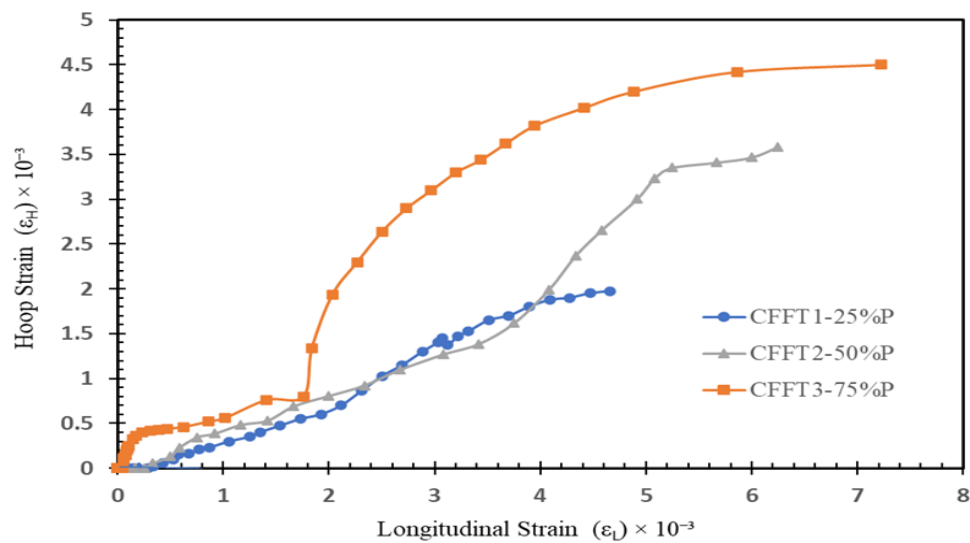


Fig. 13b. Longitudinal Strain-Hoop strain relation

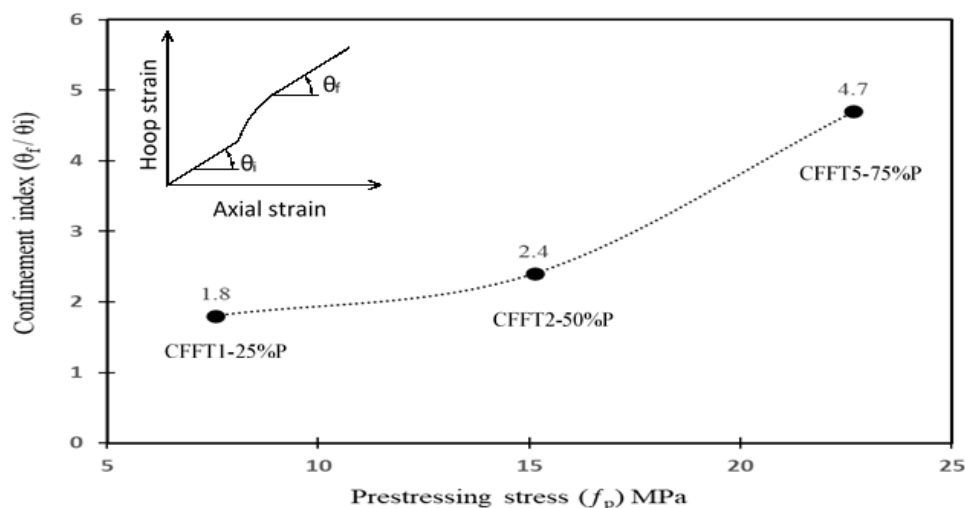
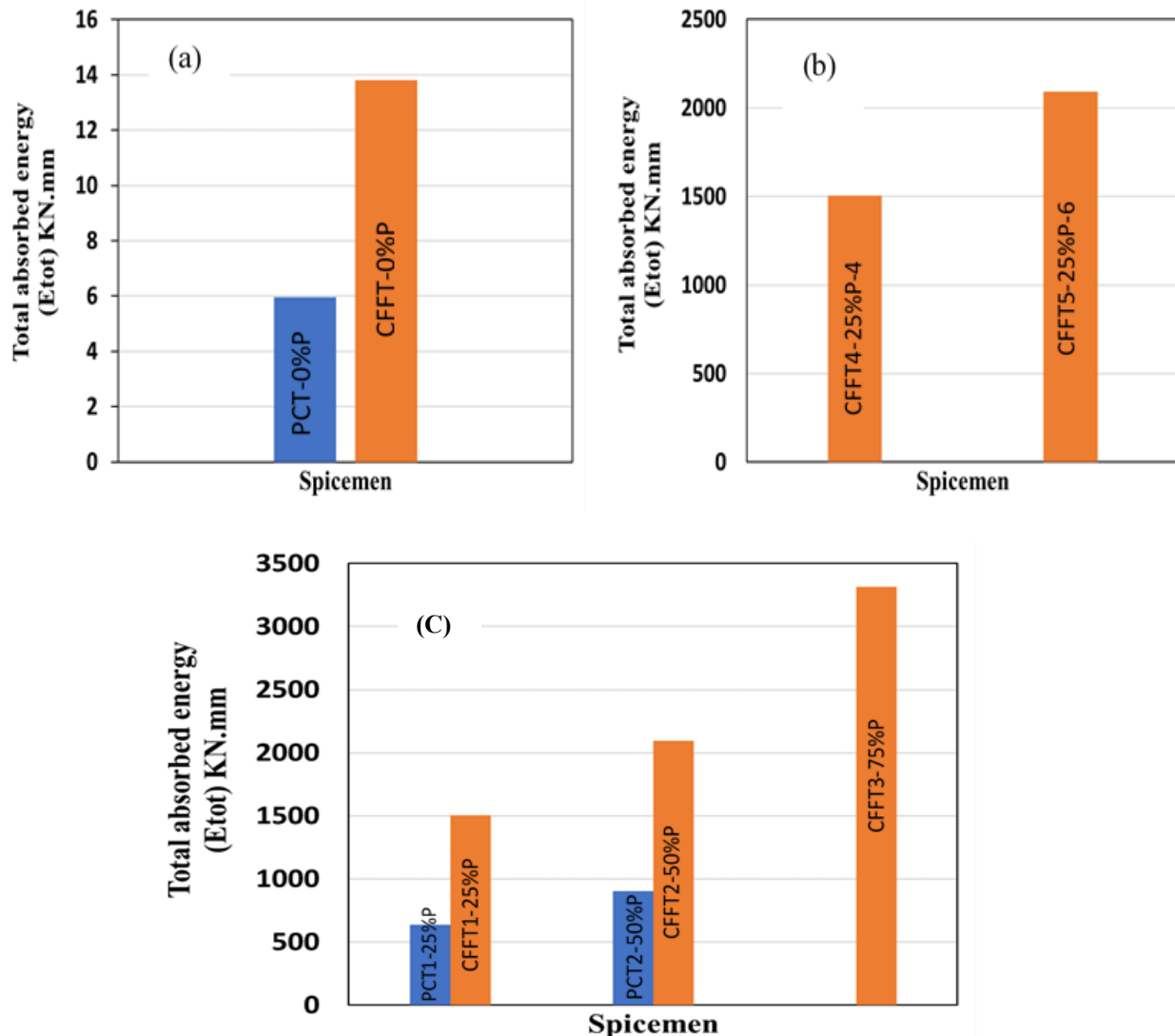


Fig. 13c. Effect of prestress level on concrete confinement

### 3.6 Ductility and energy absorption

The energy was estimated by calculating the area under load – deflection curve for each specimen. The area provided an indication of the total energy absorbed  $E_{TOT}$  by the structure or element under the applied load and could provide information about the CFFT's ductility. From **Fig. 14**, it is clear that the total absorbed energy by the specimen CFFT-0%P was higher than that of PCT-0%P, reflecting the effect of concrete confinement by the GFRP tube, that was increased by 231%, as shown in **Fig. 14a**. Furthermore, the total energy absorbed  $E_{TOT}$  was affected by the thickness of the GFRP tube; the total energy absorbed in CFFT4- 25%P-6 was higher than that in CFFT3-25%P-4, which were 27.32 KN.m and 23.18 KN.m, respectively as shown in **Fig. 14b**.

Comparing the CFFT specimens with their counterparts, PCTs, reveals an increase in the total energy absorbed, as **Fig. 14C** illustrates. The total energy absorbed increased in CFFT1-25%P and CFFT2-50%P by 250% and 247%, respectively.



**Fig. 14.** Total energy absorbed ( $E_{TOT}$ ) of specimens

## 4 Conclusions

Based on the test results and discussion presented in this study, the following conclusions can be drawn:

1. GFRP tubes are a good choice for concrete confinement. The non-corrosive tubes provide formwork, confine more concrete area than steel spirals, and contribute as longitudinal and hoop reinforcement.
2. Flexural strength and energy absorption capacities of CFFTs are considerably higher than those of PCTs. In CFFTs, the concrete cores are intact until the FRP tubes fail at substantially higher loads, either it inhibits concrete core instability from local buckling and deterioration and compression failure.



3. The thickness of the FRP tube structure wall ( $t_f$ ) has a significant effect on the CFFT strength. Increasing the fiber tube thickness in CFFT1-25%P from 2mm to 4mm and 6mm in CFFT4-25%P-4 and CFFT5-25%P-6, respectively, increasing the ultimate load by 21% and 45.3%
4. Prestressing CFFTs significantly increases their cracking strengths, initial stiffnesses, and ultimate load capacities, the ultimate failure load of specimens CFFT1-25%, CFFT2-50% and CFFT3-75% had been increased by 878%, 1156% and 1724%, respectively, by increasing axial prestressing level.
5. The confinement index ( $\theta_f / \theta_i$ ) had been derived to assess the confinement level as affected by prestressing level ( $f_p$ ), was a good assignment reflects an increase in concrete compressive strength as the prestress level increase.
6. CFFT's were provide a good ductile structure element, as the total energy absorbed ( $E_{TOT}$ ) was higher in CFFTs specimens than their counterpart in PCTs.

## References

- [1] Ahmed A Abdeldaim, Hassan M, Mohamed H, Ahmed A, Masmoudi R. Axial behavior of circular CFFT long columns internally reinforced with steel or carbon and glass FRP longitudinal bars. *Eng Struct J -Elsevier* 2018; 155:67–278.
- [2] Ahmed A Abdeldaim, Hassan M, Masmoudi R. Ultimate flexural capacity predication of rectangular FRP tube beams filled with concrete. *International Congress and Exhibition. Sustainable Civil Infrastructures, Innovative Infrastructure Geotechnology*. 2018. p. 45–55.
- [3] Ahmed A Abdeldaim, Hassan M, Masmoudi R. FRP tubes filled with reinforced concrete subjected to cyclic axial loading. *International Congress and Exhibition. Sustainable Civil Infrastructures, Innovative Infrastructure Geotechnology*. 2018. p. 32–44.
- [4] Ahmed A Abdeldaim, Masmoudi R. Axial response of concrete-filled FRP tube (CFFT) columns with internal bars. *J Compos Sci* 2018;2(4):57–70.
- [5] Roeder CW, Lehman DE, Bishop E. Strength and stiffness of circular concrete filled tubes. *J Struct Eng* 2010; 136:1545–53.
- [6] American Concrete Institute (ACI Committee 440). Guide test methods for fiber- reinforced polymers (FRPs) for reinforcing or strengthening concrete structures. ACI 440.3R-04. Farmington Hills, MI, USA; 2004. p. 40.
- [7] Fam A, Mandal SK. Prestressed concrete-filled fiber-reinforced polymer circular tubes tested in flexure. *PCI J Paper* 2006; 51:42–54.
- [8] Zhan Y, Zhao R, John Z, Xu T, Song R. Behavior of prestressed concrete-filled steel tube (CFST) beam. *J Struct Eng* 2016; 122:144–55.
- [9] ASTM D638 – 10. Standard test method for tensile properties of plastics. American National Standards Institute (ANSI), 25 W. 43rd St., 4th Floor, New York, NY 10036; 2010. <http://www.ansi.org>.